SCIENCE CHINA
Physics, Mechanics & Astronomy

• Article •

December 2017 Vol. 60 No. 12: 129511
doi: 10.1007/s11433-017-9078-5

More than six hundred new families of Newtonian periodic planar collisionless three-body orbits

XiaoMing Li[1], and ShiJun Liao[1,2*]

[1]*School of Naval Architecture, Ocean and Civil Engineering, Shanghai Jiaotong University, Shanghai 200240, China;*
[2]*MoE Key Laboratory in Scientific and Engineering Computing, Shanghai 200240, China*

Received July 4, 2017; accepted July 11, 2017; published online September 11, 2017

The famous three-body problem can be traced back to Isaac Newton in the 1680s. In the 300 years since this "three-body problem" was first recognized, only three families of periodic solutions had been found, until 2013 when Šuvakov and Dmitrašinović [Phys. Rev. Lett. **110**, 114301 (2013)] made a breakthrough to numerically find 13 new distinct periodic orbits, which belong to 11 new families of Newtonian planar three-body problem with equal mass and zero angular momentum. In this paper, we numerically obtain 695 families of Newtonian periodic planar collisionless orbits of three-body system with equal mass and zero angular momentum in case of initial conditions with isosceles collinear configuration, including the well-known figure-eight family found by Moore in 1993, the 11 families found by Šuvakov and Dmitrašinović in 2013, and more than 600 new families that have never been reported, to the best of our knowledge. With the definition of the average period $\bar{T} = T/L_{\rm f}$, where $L_{\rm f}$ is the length of the so-called "free group element", these 695 families suggest that there should exist the quasi Kepler's third law $\bar{T}^* \approx 2.433 \pm 0.075$ for the considered case, where $\bar{T}^* = \bar{T}|E|^{3/2}$ is the scale-invariant average period and E is its total kinetic and potential energy, respectively. The movies of these 695 periodic orbits in the real space and the corresponding close curves on the "shape sphere" can be found via the website: http://numericaltank.sjtu.edu.cn/three-body/three-body.htm.

three-body problem, periodic orbits, clean numerical simulation (CNS)

PACS number(s): 45.50.Jf, 05.45.-a, 95.10.Ce

Citation: X. M. Li, and S. J. Liao, More than six hundred new families of Newtonian periodic planar collisionless three-body orbits, Sci. China-Phys. Mech. Astron. **60**, 129511 (2017), doi: 10.1007/s11433-017-9078-5

1 Introduction

The famous three-body problem [1] can be traced back to Isaac Newton in the 1680s. According to Poincaré [2], a three-body system is not integrable in general. Besides, orbits of three-body problem are often chaotic [3], i.e., sensitive to initial conditions [2], although there exist periodic orbits in some special cases. In the 300 years since this "three-body problem" [1] was first recognized, only three families of periodic solutions had been found, until 2013 when Šuvakov and Dmitrašinović [4] made a breakthrough to find 13 new distinct periodic collisionless orbits belonging to 11 new families of Newtonian planar three-body problem with equal mass and zero angular momentum. Before their elegant work, only 3 families of periodic three-body orbits were found: (1) the Lagrange-Euler family discovered by Lagrange and Euler in the 18th century; (2) the Broucke-Hadjidemetriou-Hénon family [5-9]; (3) the figure-eight family, first discovered numerically by Moore [10] in 1993 and rediscovered by Chenciner and Montgomery [11] in 2000, and then extended to the rotating case [12-15]. In 2014, Li and Liao [16] studied the stability of the periodic orbits in ref. [4]. In 2015, Hudomal [17] reported 25 families of periodic orbits, including the 11 families found in ref. [4].

*Corresponding author (email: sjliao@sjtu.edu.cn)

Some studies on topological dependence of Kepler's third law for three-body problem were currently reported [18, 19].

Recently, Šuvakov and Dmitrašinović [20] specifically illustrated their numerical strategies used in ref. [4] for their 11 families of periodic orbits with the periods $T \leq 100$. They suggested that more new periodic solutions are expected to be found when $T \geq 100$. In this paper, we used a different numerical approach to solve the same problem, i.e. Newtonian planar three-body problem with equal mass and zero angular momentum, but gained 695 families of periodic orbits without collision, i.e. 229 families within $T \leq 100$ and 466 families within $100 < T \leq 200$, including the well-known figure-eight family found by Moore [10], the 11 families found by Šuvakov and Dmitrašinović [4], the 25 families mentioned in ref. [17], and especially more than 600 new families that have been never reported, to the best of our knowledge.

2 Numerical approaches

The motions of Newtonian planar three-body system are governed by the Newton's second law and gravitational law

$$\ddot{\boldsymbol{r}}_i = \sum_{j=1, j\neq i}^{3} \frac{Gm_j(\boldsymbol{r}_j - \boldsymbol{r}_i)}{|\boldsymbol{r}_i - \boldsymbol{r}_j|^3}, \tag{1}$$

where $\boldsymbol{r}_i$ and m_j are the position vector and mass of the ith body ($i, j = 1, 2, 3$), G is the Newtonian gravity coefficient, and the dot denotes the derivative with respect to the time t, respectively. Like Šuvakov and Dmitrašinović [4], we consider a planar three-body system with zero angular momentum in the case of $G = 1$, $m_1 = m_2 = m_3 = 1$, and the initial conditions in case of the isosceles collinear configurations:

$$\begin{cases} \boldsymbol{r}_1(0) = (x_1, x_2) = -\boldsymbol{r}_2(0), \quad \boldsymbol{r}_3(0) = (0, 0), \\ \dot{\boldsymbol{r}}_1(0) = \dot{\boldsymbol{r}}_2(0) = (v_1, v_2), \quad \dot{\boldsymbol{r}}_3(0) = -2\dot{\boldsymbol{r}}_1(0), \end{cases} \tag{2}$$

which are specified by the 4 parameters (x_1, x_2, v_1, v_2). Write $\boldsymbol{y}(t) = (\boldsymbol{r}_1(t), \dot{\boldsymbol{r}}_1(t))$. A periodic solution with the period T_0 is the root of the equation $\boldsymbol{y}(T_0) - \boldsymbol{y}(0) = 0$, where T_0 is unknown. Note that $x_1 = -1$ and $x_2 = 0$ correspond to the normal case considered in ref. [4] that regards $\boldsymbol{r}_1(0) = (-1, 0)$ to be fixed. However, unlike Šuvakov and Dmitrašinović [4], we regard x_1 and x_2 as variables. So, mathematically speaking, we search for the periodic orbits of the same three-body problem using a larger degree of freedom than Šuvakov and Dmitrašinović [4].

First, like Šuvakov and Dmitrašinović [4], we use the grid search method to find candidates of the initial conditions $\boldsymbol{y}(0) = (x_1, x_2, v_1, v_2)$ for periodic orbits. As is well known, the grid search method suffers from the curse of dimensionality. In order to reduce the dimension of the search space, we set the initial positions $x_1 = -1$ and $x_2 = 0$. Then, we search for the initial conditions of periodic orbits in the two dimensional plane: $v_1 \in [0, 1]$ and $v_2 \in [0, 1]$. We set 1000 points in each dimension and thus have one million grid points in the square search plane. With these different 10^6 initial conditions, the motion equations (1) subject to the initial conditions (2) are integrated up to the time $t = 100$ by means of the ODE solver dop853 developed by Hairer et al. [21], which is based on an explicit Runge-Kutta method of order 8(5,3) in double precision with adaptive step size control. The corresponding initial conditions and the period T_0 are chosen as the candidates when the return proximity function

$$|\boldsymbol{y}(T_0) - \boldsymbol{y}(0)| = \sqrt{\sum_{i=1}^{4} (y_i(T_0) - y_i(0))^2} \tag{3}$$

is less than 10^{-1}.

Second, we modify these candidates of the initial conditions by means of the Newton-Raphson method [22-24]. At this stage, the motion equations are solved numerically by means of the same ODE solver dop853 [21]. A periodic orbit is found when the level of the return proximity function (3) is less than 10^{-6}. Note that, different from the numerical approach in ref. [4], not only the initial velocity $\dot{\boldsymbol{r}}_1(0) = (v_1, v_2)$ but also the initial position $\boldsymbol{r}_1(0) = (x_1, x_2)$ are also modified. In other words, our numerical approach also allows $\boldsymbol{r}_1(0) = (x_1, x_2)$ to deviate from its initial guess $(-1, 0)$. With such kind of larger degree of freedom, our approach gives 137 families of periodic orbits, including the well-known figure-eight family [10], the 10 families found by Šuvakov and Dmitrašinović [4], and lots of completely new families that have never been reported.

However, one family reported in ref. [4] was not among these 137 periodic orbits. So, at least one periodic orbit was lost at this stage. This is not surprising, since three-body problem is not integrable in general [2] and might be rather sensitive to initial conditions, i.e., the butterfly-effect [3]. For example, Hoover et al. [25] compared numerical simulations of a chaotic Hamiltonian system given by five symplectic and two Runge-Kutta integrators in double precision, and found that "all numerical methods are susceptible", "which severely limits the maximum time for which chaotic solutions can be accurate", although "all of these integrators conserve energy almost perfectly". In fact, there exist many examples which suggest that numerical noises have great influence on chaotic systems. Currently, some numerical approaches were developed to gain reliable results of chaotic systems in a long (but finite) interval of time. One of them is the so-called "clean numerical simulation" (CNS) [26-31], which is based on the arbitrary order of Taylor series method [32-35] in arbitrary precision [36, 37], and more importantly, a check of solution

verification (in a given interval of time) by comparing two simulations gained with different levels of numerical noise.

We checked the 137 periodic orbits by means of the high-order Taylor series method in the 100-digit precision with truncation errors less than 10^{-70}, and guaranteed that they are indeed periodic orbits. Especially, we further found the additional 27 families of periodic orbits (with the periods less than 100) by means of the Newton-Raphson method [22-24] for the modifications of initial conditions and using the high-order Taylor series method (in 100-digit precision with truncation errors less than 10^{-70}) for the evolution of motion equations (1), instead of the ODE solver dop853 [21] based on the Runge-Kutta method in double precision. In addition, we use the CNS with even smaller round-off error (in 120-digit precision) and truncation error (less than 10^{-90}) to guarantee the reliability of these 27 families. It is found that one of them belongs to the 11 families found by Šuvakov and Dmitrašinović [4].

Similarly, we found 165 families within the period $100 < T_0 < 200$, including 119 families gained by the ODE solver dop853 [21] in double precision and the additional 46 families by the CNS in the multiple precision. Obviously, more periodic orbits can be found within a larger period.

It is interesting that more periodic orbits can be found by means of finer search grids. Using 2000×2000 grids for the candidates of initial conditions, we gained totally 498 periodic orbits within $0 < T_0 < 200$ in the similar way, including the 163 families within $0 \le T_0 \le 100$ by the ODE solver dop853 [21] in double precision, the additional 33 families within $0 \le T_0 \le 100$ by the CNS in the multiple precision, the 182 families within $100 < T_0 \le 200$ by the ODE solver dop853 in double precision, the additional 120 families within $100 < T_0 \le 200$ by the CNS in the multiple precision, respectively.

Similarly, using 4000×4000 grids, we totally gained 695 periodic orbits within $0 < T_0 < 200$, including the 192 families within $0 \le T_0 \le 100$ by the ODE solver dop853 [21] in double precision, the additional 37 families within $0 \le T_0 \le 100$ by the CNS in the multiple precision, the 260 families within $100 < T_0 \le 200$ by the ODE solver dop853 in double precision, and the additional 206 families within $100 < T_0 \le 200$ by the CNS in the multiple precision, respectively. Thus, the finer the search grid, the more periodic orbits can be found. It is indeed a surprise that there exist much more families of periodic orbits of three-body problem than we had thought a few years ago!

It should be emphasized that, in case of the search grid 4000×4000, we found 243 more periodic orbits by means of the CNS [26-31] in multiple precision than the ODE solver dop853 [21] in double precision. It indicates that the numerical noises might lead to great loss of periodic orbits of three-body system.

3 Periodic orbits of the three-body system

The Montgomery's topological identification and classification method [38] is used here to identify these periodic orbits. The positions $\boldsymbol{r_1}, \boldsymbol{r_2}$ and $\boldsymbol{r_3}$ of the three-body correspond to a unit vector $\boldsymbol{n}$ in the so-called "shape sphere" with the Cartesian components

$$n_x = \frac{2\boldsymbol{\rho}\cdot\boldsymbol{\lambda}}{R^2}, \quad n_y = \frac{\lambda^2-\rho^2}{R^2}, \quad n_z = \frac{2(\boldsymbol{\rho}\times\boldsymbol{\lambda})\cdot\boldsymbol{e}_z}{R^2},$$

where $\boldsymbol{\rho} = \frac{1}{\sqrt{2}}(\boldsymbol{r_1}-\boldsymbol{r_2})$, $\boldsymbol{\lambda} = \frac{1}{\sqrt{6}}(\boldsymbol{r_1}+\boldsymbol{r_2}-2\boldsymbol{r_3})$ and the hyperradius $R = \sqrt{\rho^2+\lambda^2}$. A periodic orbit of three-body system gives a closed curve on the shape sphere, which can be characterized by its topology with three punctures (two-body collision points). With one of the punctures as the "north pole", the sphere can be mapped onto a plane by a stereographic projection. And a closed curve can be mapped onto a plane with two punctures and its topology can be described by the so-called "free group element" (word) with letters a (a clockwise around right-hand side puncture), b (a counterclockwise around left-hand side puncture) and their inverses $a^{-1} = A$ and $b^{-1} = B$. For details, please refer to refs. [20,38].

The periodic orbits can be divided into different classes according to their geometric and algebraic symmetries [4]. There are two types of geometric symmetries in the shape space:

(I) the reflection symmetries of two orthogonal axes — the equator and the zeroth meridian passing through the "far" collision point;

(II) a central reflection symmetry about one point — the intersection of the equator and the aforementioned zeroth meridian.

Besides, Šuvakov and Dmitrašinović [4] mentioned three types of algebraic exchange symmetries for the free group elements:

(A) free group elements are symmetric with $a \leftrightarrow A$ and $b \leftrightarrow B$;

(B) free group elements are symmetric with $a \leftrightarrow b$ and $A \leftrightarrow B$;

(C) free group elements are not symmetric under either (A) or (B).

The 695 families of the periodic collisionless orbits can be divided into five classes: I.A, II.A, I.B, II.B and II.C, as listed in Table S. III-XXX in ref. [39]. Note that the class II.A was not included in ref. [4]. Here, we regard all periodic orbits

(and its satellites) with the same free group element as one family, so the "moth I" orbit and its satellite "yarn" orbit in ref. [4] belong to one family in this paper. These 695 families include the figure-eight family [10, 11], the 11 families found by Šuvakov and Dmitrašinović [4] (see Table a1) and the 25 families reported in ref. [17] (11 among them were given in ref. [4], see Table a2). In Tables a1 and a2, the superscript i.c. indicates the case of the initial conditions with isosceles collinear configuration, due to the fact that there exist periodic orbits in many other cases. Note that Rose [40] currently reported 90 periodic planar collisionless orbits in the same case of the isosceles collinear configurations (2), which include the figure-eight family [10, 11] and many families reported in refs. [4, 17]. Even considering these, more than 600 families among our 695 ones are new.

Note that the initial positions $\boldsymbol{r}_1 = (x_1, x_2)$ in Tables S.III-XVI in ref. [39] depart from $(-1, 0)$ a little. However, it is well-known that, if $\boldsymbol{r}_i(t)$ $(i = 1, 2, 3)$ denotes a periodic orbit with the period T of a three-body system, then

$$\boldsymbol{r}_i'(t') = \alpha\, \boldsymbol{r}_i(t), \quad \boldsymbol{v}_i'(t') = \boldsymbol{v}_i(t)/\sqrt{\alpha}, \quad t' = \alpha^{3/2}\, t \tag{4}$$

is also a periodic orbit with the period $T' = \alpha^{3/2}\, T$ for arbitrary $\alpha > 0$. Thus, through coordinate transformation and then the scaling of the spatial and temporal coordinates, we can always enforce (−1,0), (1,0) and (0,0) as the initial positions of the body 1, 2 and 3, respectively, with the initial velocities $\dot{\boldsymbol{r}}_1(0) = \dot{\boldsymbol{r}}_2(0)$ and $\dot{\boldsymbol{r}}_3(0) = -2\dot{\boldsymbol{r}}_1(0)$, corresponding to zero angular momentum. This is the reason why we choose −1 and 0 as the initial guesses of x_1 and x_2 for our search approaches. The corresponding initial velocities of the 695 periodic orbits are listed in Tables S.XVII-XXX in ref. [39]. The scatterplot of the initial velocities of the 695 periodic orbits are shown in Figure 1. Note that two very close initial conditions can give completely different periodic orbits. This well explains why more periodic orbits can be found by means of finer search grids.

The so-called "free group elements" of these 695 families are listed in Tables S.XXXI-LIV in ref. [39]. Due to the limited length, only six newly-found ones are listed in Table 1, and their real space orbits are shown in Figure 2. In addition, the real space orbits of a few families are shown in Figure a1. The movies of these 695 periodic orbits in the real space and the corresponding close curves on the shape sphere can be found via the website: http://numericaltank.sjtu.edu.cn/three-body/three-body.htm.

For a two-body system, there exists the so-called Kepler's third law $r_a \propto T^{2/3}$, where T is the period and r_a is the semi-major axis of periodic orbit. For a three-body system, Šuvakov and Dmitrašinović [4] mentioned that there should exist the relation $T^{2/3}|E| =$ constant, where E denotes the total kinetic and potential energy of the three-body system. But, they pointed out that "the constant on the right-hand side of this equation is not universal", which may depend on "both of the family of the three-body orbit and its angular momentum" [4]. However, with the definition of the average period $\bar{T} = T/L_{\rm f}$, where $L_{\rm f}$ is the length of free group element of

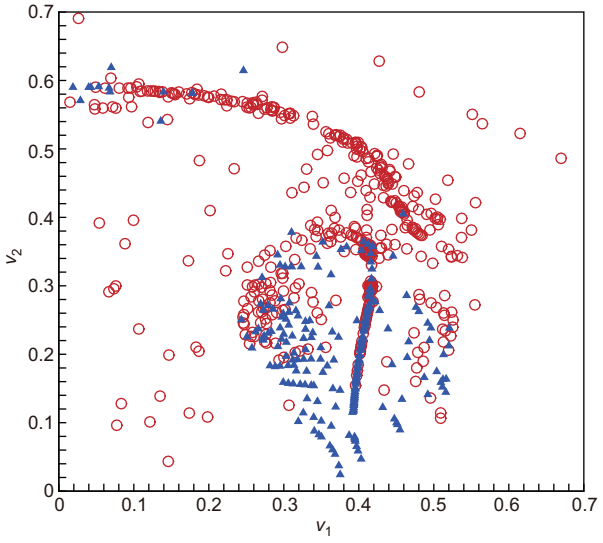

Figure 1 (Color online) The scatterplot of the initial velocities of the 695 periodic orbits. Circle: the orbits gained by ODE solver dop853 in double precision; triangle: the orbits gained by the CNS in the multiple precision.

Table 1 The initial velocities and periods T of some newly-found periodic orbits of the three-body system with equal mass and zero angular momentum in the case of the isosceles collinear configurations: $\boldsymbol{r}_1(0) = (-1, 0) = -\boldsymbol{r}_2(0)$, $\dot{\boldsymbol{r}}_1(0) = (v_1, v_2) = \dot{\boldsymbol{r}}_2(0)$ and $\boldsymbol{r}_3(0) = (0, 0)$, $\dot{\boldsymbol{r}}_3(0) = (-2v_1, -2v_2)$ when $G = 1$ and $m_1 = m_2 = m_3 = 1$, where $T^* = T|E|^{3/2}$ is its scale-invariant period, $L_{\rm f}$ is the length of the free group element. Here, the superscript i.c. indicates the case of the initial conditions with isosceles collinear configuration, due to the fact that there exist periodic orbits in many other cases

Class and number	v_1	v_2	T	T^*	$L_{\rm f}$
$\mathrm{I.A}_{77}^{\mathrm{i.c.}}$	0.4159559963	0.2988672319	114.5882843578	256.902	104
$\mathrm{I.A}_{100}^{\mathrm{i.c.}}$	0.0670760777	0.5889627892	163.9101889958	284.971	124
$\mathrm{I.A}_{115}^{\mathrm{i.c.}}$	0.3369172422	0.2901238678	139.2379425543	366.661	148
$\mathrm{I.B}_{102}^{\mathrm{i.c.}}$	0.4784306757	0.3771895698	199.5148149879	325.727	134
$\mathrm{I.B}_{155}^{\mathrm{i.c.}}$	0.3310536467	0.1351316515	192.5759642513	592.936	238
$\mathrm{II.C}_{156}^{\mathrm{i.c.}}$	0.3231926176	0.3279135713	145.3798952880	369.993	150

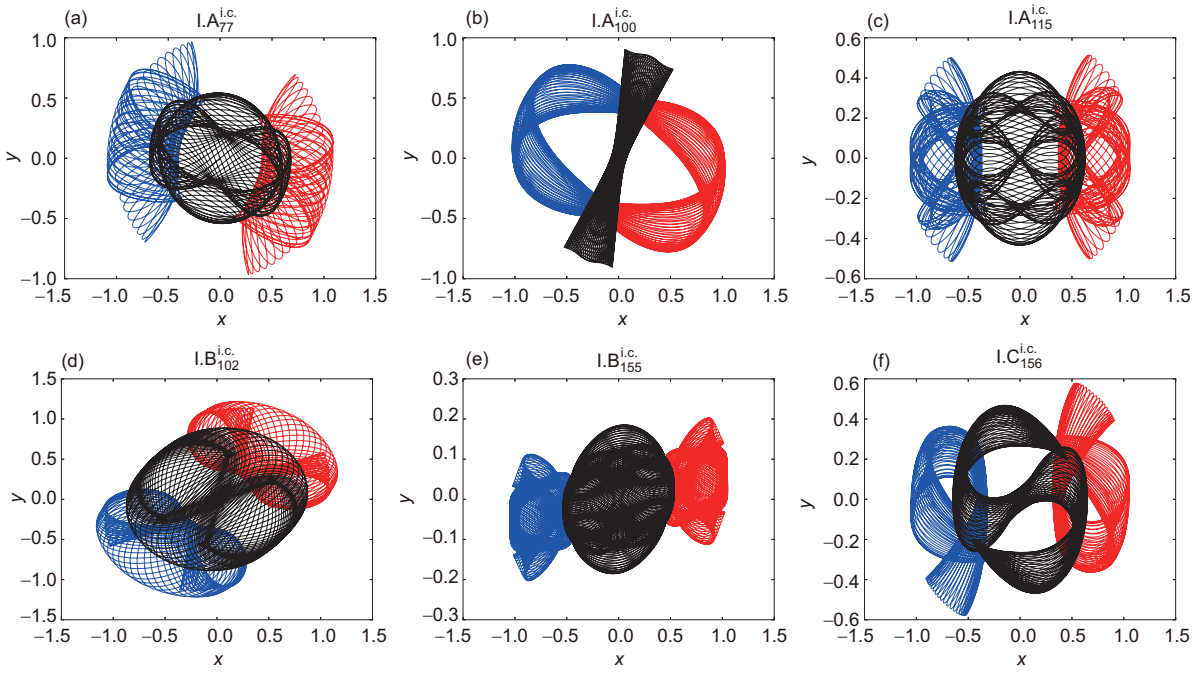

Figure 2 (Color online) Brief overview of the six newly-found families of periodic three-body orbits in case of equal mass, zero angular momentum and initial conditions with isosceles collinear configuration. Blue line, orbit of Body-1; red line, orbit of Body-2; black line, orbit of Body-3.

periodic orbit of a three-body system, the 695 families of periodic planar collisionless orbits approximately satisfy such a generalised Kepler's third law $\bar{R} \propto |E|^{-1} = 0.56\ \bar{T}^{2/3}$, as shown in Figure 3, where $\bar{R}$ is the mean of hyper-radius of the three-body system. In other words, the scale-invariant average period $\bar{T}^* = \bar{T}|E|^{3/2}$ should be approximately equal to a universal constant, i.e. $\bar{T}^* \approx 2.433 \pm 0.075$, for the three-body system with equal mass and zero angular momentum in the case of initial conditions with isosceles collinear configurations (2). Note that the scale-invariant period $T^* = T|E|^{3/2}$ and $L_{\rm f}$ (the length of free group element) are invariable under the scaling (4) of the spatial and temporal coordinates for arbitrary $\alpha > 0$. So, they are two characteristics with important physical meanings for each family that contains an infinite number of periodic orbits corresponding to different scaling parameters $\alpha > 0$ in eq. (4).

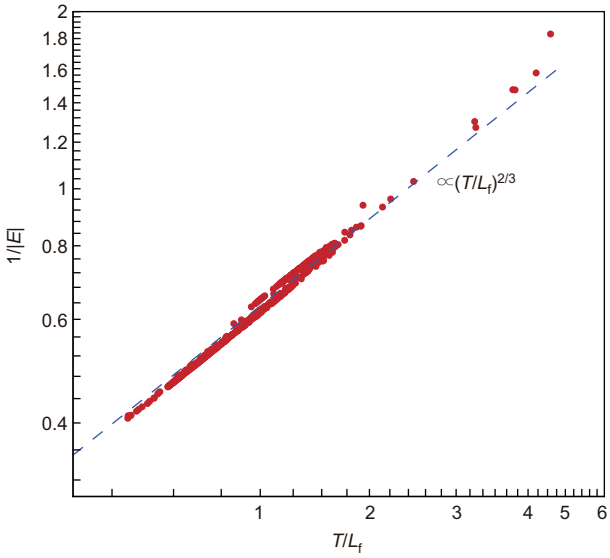

Figure 3 (Color online) The inverse of total energy $1/|E|$ and average period $T/L_{\rm f}$ approximately fall in with a power law with exponent 2/3, where $L_{\rm f}$ is the length of free group element. Symbols: the 695 families of periodic orbits; dashed line: $1/|E| = 0.56 \cdot (T/L_{\rm f})^{2/3}$.

4 Conclusions

In this paper, we gain 695 families of periodic orbits of the three-body system with equal mass, zero angular momentum and initial conditions in the isosceles collinear configuration $\boldsymbol{r}_1 = (-1, 0), \boldsymbol{r}_2 = (+1, 0), \boldsymbol{r}_3 = (0, 0)$. These 695 families include the figure-eight family [10,11], the 11 families found by Šuvakov and Dmitrašinović [4] (see Table a1) and the 25 families reported in ref. [17] (11 among them were given in ref. [4], see Table a2). Especially, more than six hundreds among them are completely new and have been never reported, to the best of our knowledge. It should be emphasized that 243 more periodic orbits are found by means of the CNS [26-31] in multiple precision than the ODE solver dop853 [21] in double precision. This indicates the great potential of the CNS for complicated nonlinear dynamic systems.

It should be emphasized that, in the considered initial conditions with isosceles collinear configuration, more and more periodic planar three-body orbits could be found by means of finer search grids within a larger period. Similarly, a large number of periodic orbits can be gained in other cases of three-body systems. Thereafter, a data base for periodic orbits of three-body problem could be built, which is of benefit to better understandings of three-body systems, a very famous problem that can be traced back to Isaac Newton in the 1680s.

This work was partly supported by the National Natural Science Foundation of China (Grant No. 11432009). This work was carried out on TH-2 at National Supercomputer Centre in Guangzhou, China.

1 Z. E. Musielak, and B. Quarles, Rep. Prog. Phys. **77**, 065901 (2014).
2 H. Poincaré, Acta Math. **13**, 5 (1890).
3 E. N. Lorenz, J. Atmos. Sci. **20**, 130 (1963).
4 M. Šuvakov, and V. Dmitrašinović, Phys. Rev. Lett. **110**, 114301 (2013).
5 R. Broucke, Celestial Mech. **12**, 439 (1975).
6 J. D. Hadjidemetriou, Celestial Mech. **12**, 255 (1975).
7 J. D. Hadjidemetriou, and T. Christides, Celestial Mech. **12**, 175 (1975).
8 M. Hénon, Celestial Mech. **13**, 267 (1976).
9 M. Hénon, Celestial Mech. **15**, 243 (1977).
10 C. Moore, Phys. Rev. Lett. **70**, 3675 (1993).
11 A. Chenciner, and R. Montgomery, Ann. Math. **152**, 881 (2000).
12 M. Nauenberg, Phys. Lett. A **292**, 93 (2001).
13 A. Chenciner, J. Féjoz, and R. Montgomery, Nonlinearity **18**, 1407 (2005).
14 R. Broucke, A. Elipe, and A. Riaguas, Chaos Soliton. Fract. **30**, 513 (2006).
15 M. Nauenberg, Celestial Mech. Dyn. Astr. **97**, 1 (2007).
16 X. M. Li, and S. J. Liao, Sci. China-Phys. Mech. Astron. **57**, 2121 (2014).
17 A. Hudomal, *New Periodic Solutions to the Three-body Problem and Gravitational Waves*, Dissertation for Master Degree (University of Belgrade, Serbia, 2015).
18 V. Dmitrašinović, and M. Šuvakov, Phys. Lett. A **379**, 1939 (2015).
19 M. R. Janković, and V. Dmitrašinović, Phys. Rev. Lett. **116**, 064301 (2016).
20 M. Šuvakov, and V. Dmitrašinović, Am. J. Phys. **82**, 609 (2014).
21 E. Hairer, S. P. Nørsett, and G. Wanner, *Solving Ordinary Differential Equations I: Nonstiff Problems* (Springer-Verlag, Berlin, 1993).
22 S. C. Farantos, J. Mol. Struc.-Theochem **341**, 91 (1995).
23 M. Lara, and J. Peláez, Astron. Astrophys. **389**, 692 (2002).
24 A. Abad, R. Barrio, and Dena, Phys. Rev. E **84**, 016701 (2011).
25 W. G. Hoover, and C. G. Hoover, Comput. Meth. Sci. Tech. **21**, 109 (2015).
26 S. Liao, Tellus A **61**, 550 (2008).
27 S. Liao, Commun. Nonlinear Sci. Numer. Simul. **19**, 601 (2014).
28 S. Liao, Chaos Soliton. Fract. **47**, 1 (2013).
29 S. J. Liao, and P. F. Wang, Sci. China-Phys. Mech. Astron. **57**, 330 (2014).
30 S. Liao, and X. Li, Int. J. Bifurcat. Chaos **25**, 1530023 (2015).
31 Z. L. Lin, L. P. Wang, and S. J. Liao, Sci. China-Phys. Mech. Astron. **60**, 014712 (2017).
32 D. Barton, Comput. J. **14**, 243 (1971).
33 G. Corliss, and Y. F. Chang, ACM Trans. Math. Softw. **8**, 114 (1982).
34 Y. F. Chang, and G. Corliss, Comput. Math. Appl. **28**, 209 (1994).
35 R. Barrio, F. Blesa, and M. Lara, Comput. Math. Appl. **50**, 93 (2005).
36 O. Portilho, Comput. Phys. Commun. **59**, 345 (1990).
37 D. Viswanath, Physica D **190**, 115 (2004).
38 R. Montgomery, Nonlinearity **11**, 363 (1998).
39 X. Li, and S. Liao, arXiv: 1705.00527.
40 D. Rose, *Geometric Phase and Periodic Orbits of the Equalmass, Planar Three-body Problem with Vanishing Angular Momentum*, Dissertation for Doctoral Degree (University of Sydney, Sydney, 2016).

Appendix

Table a1 The figure-eight and the periodic orbits reported in ref. [4] and their names defined in this paper

Class and name	Free group element	Class and number in this paper
I.A figure-eight	$abAB$	$\mathrm{I.A}_{1}^{\mathrm{i.c.}}$
I.A butterfly I and II	$(ab)^2(AB)^2$	$\mathrm{I.A}_{2}^{\mathrm{i.c.}}$
I.A bumblebee	$b^2(ABab)^2A^2(baBA)^2baB^2(abAB)^2a^2(BAba)^2BA$	$\mathrm{I.A}_{17}^{\mathrm{i.c.}}$
I.B moth I	$baBABabABA$	$\mathrm{I.B}_{1}^{\mathrm{i.c.}}$
I.B butterfly III	$(ab)^2(ABA)(ba)^2(BAB)$	$\mathrm{I.B}_{2}^{\mathrm{i.c.}}$
I.B moth II	$(abAB)^2A(baBA)^2B$	$\mathrm{I.B}_{5}^{\mathrm{i.c.}}$
I.B moth III	$ABabaBABabaBAbabABAbab$	$\mathrm{I.B}_{6}^{\mathrm{i.c.}}$
I.B goggles	$(ab)^2ABBA(ba)^2BAAB$	$\mathrm{I.B}_{3}^{\mathrm{i.c.}}$
I.B butterfly IV	$((ba)^2(AB)^2)^6A((ba)^2(BA)^2)^6B$	$\mathrm{I.B}_{49}^{\mathrm{i.c.}}$
I.B dragonfly	$b^2(ABabAB)a^2(BAbaBA)$	$\mathrm{I.B}_{4}^{\mathrm{i.c.}}$
II.C yin-yang I (a) and (b)	$(ab)^2ABAba(BAB)$	$\mathrm{II.C}_{1}^{\mathrm{i.c.}}$
II.C yin-yang II (a) and (b)	$(abaBAB)^3abaBAbab(ABAbab)^3(AB)^2$	$\mathrm{II.C}_{27}^{\mathrm{i.c.}}$

Table a2 The 14 among 25 families reported in ref. [17] and their names defined in this paper. The other 11 families was the same as listed in Table a1

Class and name in ref. [17]	Class and number in this paper	Class and name in ref. [17]	Class and number in this paper
I.5.A	$\mathrm{I.A}_{5}^{\mathrm{i.c.}}$	IVa.8.A	$\mathrm{I.B}_{13}^{\mathrm{i.c.}}$
I.8.A	$\mathrm{I.A}_{10}^{\mathrm{i.c.}}$	IVb.11.A	$\mathrm{I.B}_{17}^{\mathrm{i.c.}}$
I.12.A	$\mathrm{I.A}_{21}^{\mathrm{i.c.}}$	IVb.15.A	$\mathrm{I.B}_{59}^{\mathrm{i.c.}}$
II.6.A	$\mathrm{I.B}_{7}^{\mathrm{i.c.}}$	IVb.19.A	$\mathrm{I.B}_{38}^{\mathrm{i.c.}}$
II.8.A	$\mathrm{II.C}_{10}^{\mathrm{i.c.}}$	IVc.12.A.β	$\mathrm{II.C}_{29}^{\mathrm{i.c.}}$
III.15.A.β	$\mathrm{II.C}_{35}^{\mathrm{i.c.}}$	IVc.17.A	$\mathrm{I.B}_{33}^{\mathrm{i.c.}}$
IVa.6.A	$\mathrm{I.B}_{8}^{\mathrm{i.c.}}$	IVc.19.A	$\mathrm{I.B}_{37}^{\mathrm{i.c.}}$

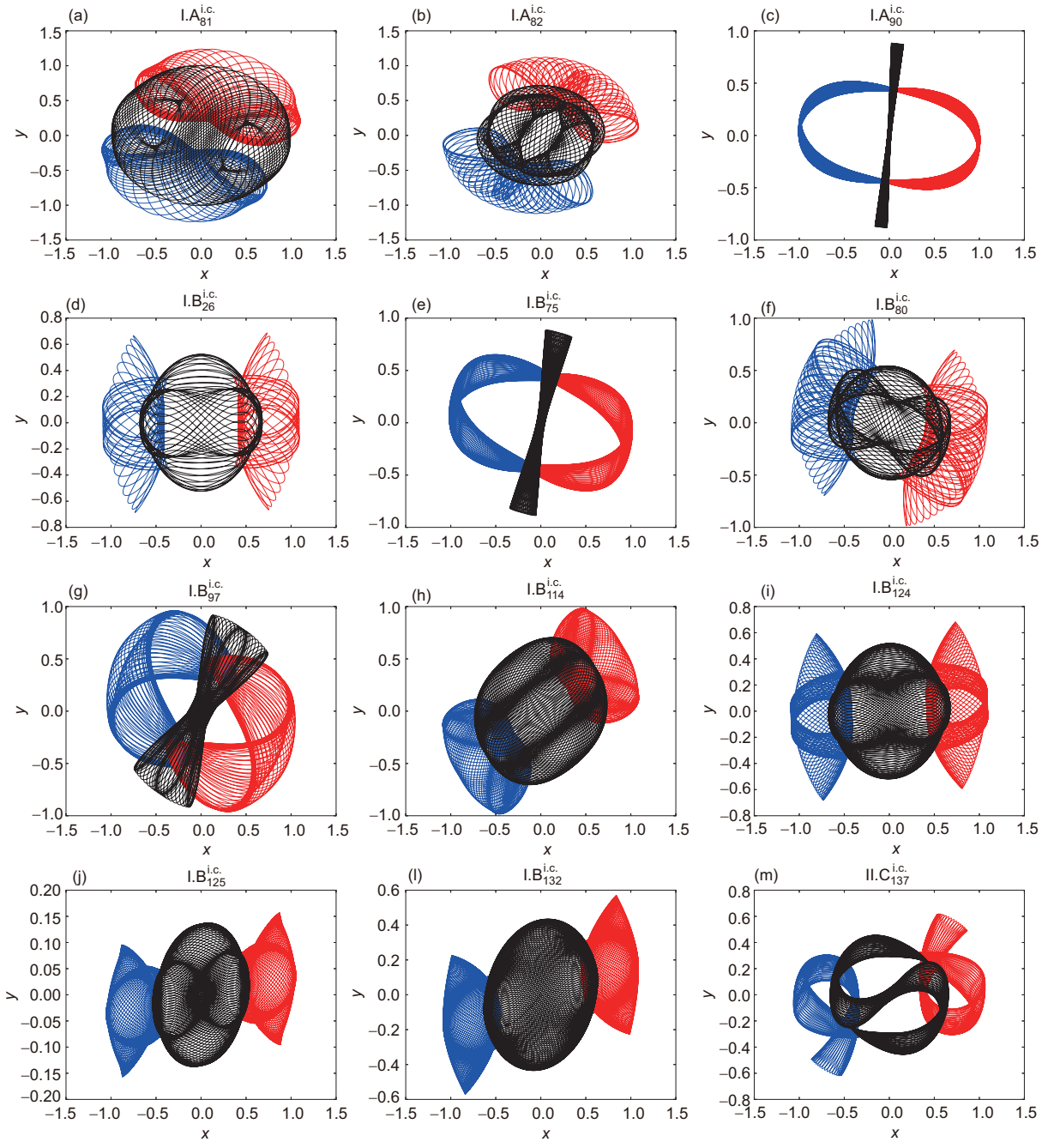

Figure a1 (Color online) Periodic orbits of the three-body system in the case of the isosceles collinear configurations: $\boldsymbol{r}_1(0) = (-1, 0) = -\boldsymbol{r}_2(0)$, $\dot{\boldsymbol{r}}_1(0) = (v_1, v_2) = \dot{\boldsymbol{r}}_2(0)$ and $\boldsymbol{r}_3(0) = (0, 0)$, $\dot{\boldsymbol{r}}_3(0) = (-2v_1, -2v_2)$, where $G = 1$ and $m_1 = m_2 = m_3 = 1$. Blue line, orbit of Body-1; red line, orbit of Body-2; black line, orbit of Body-3.